An Analysis of the Scalar Helmholtz Equation Using the Integral Equation Method

Masanori Tsuchimoto, Atsuhiko Yoneta, Toshihisa Honma, and Kenzo Miya

Abstract—**The scalar Helmholtz equations are investigated by using the integral equation method (IEM). In the IEM analysis, the fundamental solution of the Laplace equation is used as a weighting function. Two IEM formulations are obtained; one is a standard formulation and the other is obtained from an elimination of the unknown boundary value. The accuracy and computational time of the IEM are compared with those of the finite element method in two dimensional scalar Helmholtz problems. The analysis of a resonant cavity is reduced to a simple eigenvalue problem. Resonant frequencies of the IEM agree well with those of the finite difference method. Usefulness of the IEM is confirmed through the analyses of the scalar Helmholtz equations.**

I. Introduction

The GOVERNING equations for analysis of wave guides and resonant cavities are the Helmholtz wave equations. They were studied by many authors with the finite difference method (FDM) and the finite element method (FEM) [1]–[4]. When the boundary element method (BEM) is applied to the analysis, a determinant search method should be used to obtain resonant wave numbers [5]. In the determinant search method, a large number of recalculations of matrix elements are necessary for different wave numbers, since the fundamental solution of the Helmholtz equation includes the wave number. The integral equation method (IEM) makes up for this weak point of the BEM, and its usefulness is reported in analyses of eigenvalue problems [5]–[9]. Numerical formulation of the IEM is based on the BEM and the Helmholtz-wave equation is treated as the Laplace equation with an inhomogeneous term. The determinant search method is not needed in the IEM, since the fundamental solution of the Laplace equation is used as a weighting function.

In the present paper, two IEM formulations are obtained for the scalar Helmholtz equation. One is a standard formulation [5] and the other is obtained from an elimination of the unknown boundary value [8], [9]. The IEM solutions are in good agreement with exact solutions in two dimensional scalar Helmholtz problems [10], [11]. Though the IEM requires considerable computational time compared with the FEM, the first derivative is obtained directly with high accuracy. The analysis of an axisymmetric resonant cavity is reduced to a simple eigenvalue problem. Resonant frequencies agree well with the FDM solutions [1]. It is shown that the IEM is useful in solving the scalar Helmholtz equation.

Manuscript received September 19, 1990; revised August 15, 1991.
M. Tsuchimoto and K. Miya are with the Nuclear Engineering Research Laboratory, Faculty of Engineering, University of Tokyo, Tokai, Ibaraki, 319-11, Japan.
A. Yoneta and T. Honma are with the Department of Electrical Engineering, Faculty of Engineering, Hokkaido University, Sapporo, 060, Japan.
IEEE Log Number 9103893.

II. The IEM Formulation

Through a formulation of the following scalar equation, the IEM is explained:

$$\nabla^2 \phi + \alpha\phi + g = 0, \tag{1}$$

where α is a constant and g is an arbitrary function without including ϕ. A weighted residual procedure with a weighting function w is applied to (1). After integrating by parts twice, the following equation is obtained:

$$\int_\Gamma w\nabla\phi \, d\Gamma - \int_\Gamma \phi\nabla w \, d\Gamma + \int_\Omega \phi(\nabla^2 + \alpha) w \, d\Omega + \int_\Omega gw \, d\Omega = 0. \tag{2}$$

where Γ is a boundary of a domain Ω. In the IEM analysis, (1) is treated as the Laplace equation with inhomogeneous terms and the following fundamental solution ϕ^* of the Laplace equation is chosen as the weighting function w:

$$\nabla^2 \phi^* + \delta = 0, \tag{3}$$

where δ is the Dirac delta function. Then the integral equation with domain integrations is obtained for a field point i:

$$C_i\phi_i + \fint_\Gamma \phi \frac{\partial \phi^*}{\partial n} d\Gamma - \fint_\Gamma \phi^* \frac{\partial \phi}{\partial n} d\Gamma = \int_\Omega \alpha\phi\phi^* \, d\Omega + \int_\Omega g\phi^* \, d\Omega, \tag{4}$$

where $\fint$ denotes the Cauchy principal value integration. When the boundary Γ is sufficiently smooth, the coefficient C_i at the field point is evaluated as follows:

$$C_i = \begin{cases} 0 & \cdots \; i \notin \Gamma + \Omega, \\ 1/2 & \cdots \; i \in \Gamma, \\ 1 & \cdots \; i \in \Omega. \end{cases} \tag{5}$$

The boundary and the domain are divided into N and M elements, respectively. When the Dirichlet boundary condition $\phi_\Gamma = \bar{\phi}_\Gamma$ and the Neumann boundary condition $(\partial\phi/\partial n)_\Gamma = \bar{q}_\Gamma$ are applied to (4), the following matrix equations are obtained for both boundary points and internal points, respectively:

$$[C_{i\Gamma}\boldsymbol{I} + \boldsymbol{H}_\Gamma]\begin{Bmatrix}\bar{\phi}_\Gamma\\ \phi_\Gamma\end{Bmatrix} - [\boldsymbol{G}_\Gamma]\begin{Bmatrix}\bar{q}_\Gamma\\ q_\Gamma\end{Bmatrix} = [\boldsymbol{D}_\Gamma]\{\phi_\Omega\} + \{d_\Gamma\}, \quad (6)$$

$$\{\phi_i\} + [\boldsymbol{H}_\Omega]\begin{Bmatrix}\phi_\Gamma\\ \bar{\phi}_\Gamma\end{Bmatrix} - [\boldsymbol{G}_\Omega]\begin{Bmatrix}\bar{q}_\Gamma\\ q_\Gamma\end{Bmatrix} = [\boldsymbol{D}_\Omega]\{\phi_\Omega\} + \{d_\Omega\}, \quad (7)$$

$$H_{ij} = \int_{\Gamma_j} \frac{\partial\phi^*}{\partial n}\, d\Gamma, \quad G_{ij} = \int_{\Gamma_j} \phi^*\, d\Gamma,$$

$$D_{ij} = \int_{\Omega_j} \alpha\phi^*\, d\Omega, \quad d_i = \sum \int_{\Omega_j} g\phi^*\, d\Omega,$$

where $\boldsymbol{I}$ is an unit matrix. In the BEM analysis, (6) is solved to obtain unknown boundary value $\{\phi_\Gamma\}$ and $\{q_\Gamma\}$, and the internal value $\{\phi_i\}$ is calculated from (7). On the other hand, since $\{\phi_\Omega\}$ in (6) is also unknown value in the IEM analysis, positions and numbers of $\{\phi_i\}$ in the domain Ω are coincided with those of $\{\phi_\Omega\}$. Then (6) is combined with (7) to make the following simultaneous equation:

$$\begin{bmatrix} C_{i\Gamma}\boldsymbol{I} + \boldsymbol{H}_\Gamma & -\boldsymbol{G}_\Gamma & -\boldsymbol{D}_\Gamma \\ \boldsymbol{H}_\Omega & -\boldsymbol{G}_\Omega & \boldsymbol{I} - \boldsymbol{D}_\Omega \end{bmatrix}\begin{Bmatrix}\phi_\Gamma\\ q_\Gamma\\ \phi_\Omega\end{Bmatrix} = \begin{bmatrix} \boldsymbol{G}_\Gamma & -C_{i\Gamma}\boldsymbol{I} - \boldsymbol{H}_\Gamma \\ \boldsymbol{G}_\Omega & -\boldsymbol{H}_\Omega \end{bmatrix}\begin{Bmatrix}\bar{q}_\Gamma\\ \bar{\phi}_\Gamma\end{Bmatrix} + \begin{Bmatrix}d_\Gamma\\ d_\Omega\end{Bmatrix}. \quad (8)$$

This is the first IEM formulation [5]. The matrix of the left hand side (LHS) is an $(N + M) \times (N + M)$ matrix. The first derivative in Ω is calculated directly as a derivative of (4):

$$\frac{\partial\phi}{\partial x} = \int_\Gamma \frac{\partial\phi^*}{\partial x}\frac{\partial\phi}{\partial n}\, d\Gamma - \int_\Gamma \phi\,\frac{\partial}{\partial x}\frac{\partial\phi^*}{\partial n}\, d\Gamma + \int_\Omega \alpha\phi\,\frac{\partial\phi^*}{\partial x}\, d\Omega + \int_\Omega g\,\frac{\partial\phi^*}{\partial x}\, d\Omega. \quad (9)$$

Furthermore, unknown boundary value $\{^{\phi_\Gamma}_{q_\Gamma}\}$ is eliminated from (8) [8], [9]. For a simple explanation, (6) and (7) are arranged as follows:

$$[\boldsymbol{P}]\{e_\Gamma\} = [\boldsymbol{Q}]\{\bar{e}_\Gamma\} + [\boldsymbol{S}]\{\phi_\Omega\} + \{s\}, \quad (10)$$

$$\{\phi_i\} = [\boldsymbol{E}]\{e_\Gamma\} + [\boldsymbol{F}]\{\bar{e}_\Gamma\} + [\boldsymbol{T}]\{\phi_\Omega\} + \{t\} \quad (11)$$

where $\{e_\Gamma\}$ is the unknown boundary value $\{^{\phi_\Gamma}_{q_\Gamma}\}$ and $\{\bar{e}_\Gamma\}$ is the boundary condition $\{^{q_\Gamma}_{\phi_\Gamma}\}$. Since the matrix $[\boldsymbol{P}]$ in (10) is a square matrix, there is an inverse matrix

$$\{e_\Gamma\} = [\boldsymbol{P}]^{-1}([\boldsymbol{Q}]\{\bar{e}_\Gamma\} + [\boldsymbol{S}]\{\phi_\Omega\} + \{s\}). \quad (12)$$

Substitution of (12) to (11) yields

$$\{\phi_i\} = [\boldsymbol{E}][\boldsymbol{P}]^{-1}([\boldsymbol{Q}]\{\bar{e}_\Gamma\} + [\boldsymbol{S}]\{\phi_\Omega\} + \{s\}) + [\boldsymbol{F}]\{\bar{e}_\Gamma\} + [\boldsymbol{T}]\{\phi_\Omega\} + \{t\}. \quad (13)$$

When $\{\phi_i\}$ is coincided with $\{\phi_\Omega\}$, (13) is expressed as

$$([\boldsymbol{I}] - [\boldsymbol{E}][\boldsymbol{P}]^{-1}[\boldsymbol{S}] - [\boldsymbol{T}])\{\phi_\Omega\} = ([\boldsymbol{E}][\boldsymbol{P}]^{-1}[\boldsymbol{Q}] + [\boldsymbol{F}])\{\bar{e}_\Gamma\} + [\boldsymbol{E}][\boldsymbol{P}]^{-1}\{s\} + \{t\}. \quad (14)$$

This is the second IEM formulation, where the matrix of the LHS is an $M \times M$ matrix.

III. Numerical Results and Discussion

A. Analysis of Two Dimensional Scalar Helmholtz Equation

Recently, stabilities of vector FEM solutions are discussed in eddy current analyses [10], [11]. The problem and its boundary condition are defined as follows in two dimensional Cartesian coordinates (x, y) [10]:

$$\nabla \times \nabla \times \boldsymbol{B} + \lambda\boldsymbol{B} = \boldsymbol{f} \text{ in } \Omega, \quad \boldsymbol{n} \times \boldsymbol{B} = \boldsymbol{0} \text{ on } \Gamma,$$

$$\boldsymbol{f} = \{2 + \lambda(y - y^2)\}\boldsymbol{i} + \{2 + \lambda(x - x^2)\}\boldsymbol{j}, \quad (15)$$

where $\boldsymbol{B}$, $\boldsymbol{n}$ are the magnetic field and a normal unit vector on Γ, and $\boldsymbol{i}$, $\boldsymbol{j}$ indicate an unit vector for x, y directions. The coefficient λ is a time constant in the eddy current analyses [10], [11]. In this section, (15) is transformed to scalar Helmholtz equations and the IEM is applied to analyses of the scalar equations. The exact solution of (15) is obtained for a square numerical model in Fig. 1 [10]:

$$\boldsymbol{B} = (y - y^2)\boldsymbol{i} + (x - x^2)\boldsymbol{j}, \quad (16)$$

Fig. 2 shows distributions of the exact solutions. From the boundary condition in (15), the magnetic field is perpendicular to the boundary of the model. Equation (15) is transformed as follows under a condition of $\nabla \cdot \boldsymbol{B} = \boldsymbol{0}$:

$$\nabla^2\boldsymbol{B} - \lambda\boldsymbol{B} = -\boldsymbol{f}. \quad (17)$$

For the numerical model in Fig. 1, (17) is separated into x, y components and reduced to the following scalar equations:

$$\nabla^2 B_x - \lambda B_x = -2 - \lambda(y - y^2),$$

$$\nabla^2 B_y - \lambda B_y = -2 - \lambda(x - x^2), \quad (18)$$

Furthermore, an equivalent scalar Helmholtz equation to (15) and its boundary condition are obtained from $\boldsymbol{B} = \nabla \times \boldsymbol{A}$, $\boldsymbol{A} = (0, 0, A_z)$ [11]:

$$\nabla^2 A_z - \lambda A_z = -g, \quad \text{in } \Omega, \quad \partial A_z/\partial n = 0 \text{ on } \Gamma,$$

$$g = 2(y - x) + \lambda[\tfrac{1}{2}(y^2 - x^2) - \tfrac{1}{3}(y^3 - x^3)\}. \quad (19)$$

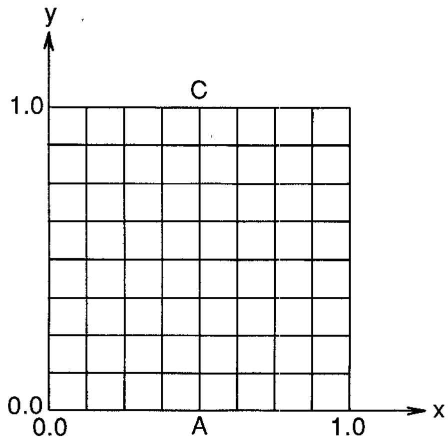

Fig. 1. Division of the numerical model for the two dimensional scalar Helmholtz equation.

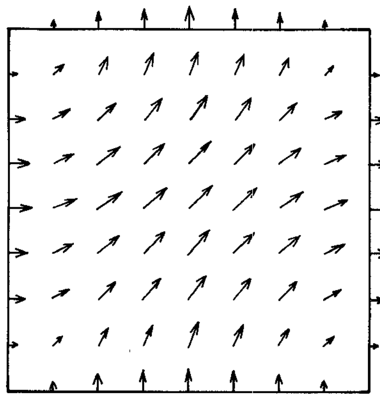

Fig. 2. Distributions of exact solutions of (16).

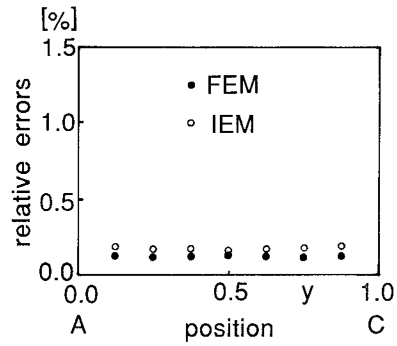

Fig. 3. Relative errors of the IEM and the FEM solutions of (18) on the line AC in Fig. 1.

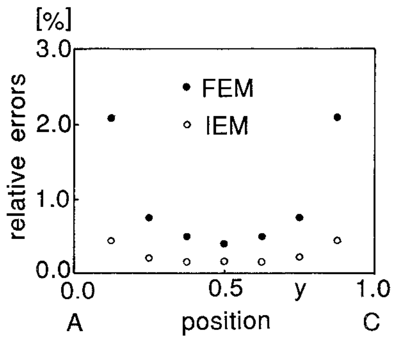

Fig. 4. Relative errors of the IEM and the FEM solutions of (19) on the line AC in Fig. 1.

Equations (18) and (19) are solved by the IEM and the FEM. The same evaluation of the integrals is applied in order to compare results of the both methods. The model in Fig. 1 is divided to 8 × 8 domain elements and the integrals are evaluated by using the Gaussian integration with linear interpolation functions. Fig. 3 shows relative errors of the magnetic field B_x of (18) on the line AC in Fig. 1. The coefficient λ is set to 10^{-6} which is a typical parameter for spurious solutions in the vector FEM analyses [10], [11]. Since (18) is a scalar equation, there is no spurious solution in the analysis [10], [11]. Both IEM and FEM solutions agree well with exact solutions. In the analysis of (19), the magnetic field B_x is obtained as the derivative of A_z, i.e., $B_x = (\partial A_z/\partial y)$. Relative errors are shown in Fig. 4. In the standard FEM analyses, the first derivative is calculated as a difference of internal values. A rough division of the model often becomes a source of error. In the IEM, the first derivative is obtained directly from (9) with high accuracy. On the other hand, computational time of the IEM is about twice as long as that of the FEM, since integrals are complicated in the IEM compared with those in the FEM.

B. Analysis of an Axisymmetric Resonant Cavity

In this section, an axisymmetric resonant cavity is studied with the second IEM formulation. Maxwell's equations are expressed by the following vector Helmholtz equations for a resonant cavity with perfect conducting walls:

$$\nabla \times \nabla \times \boldsymbol{H} = k^2\boldsymbol{H}, \quad \nabla \times \nabla \times \boldsymbol{E} = k^2\boldsymbol{E}, \tag{20}$$

where $\boldsymbol{H}$, $\boldsymbol{E}$, k are the magnetic field, the electric field and a wave number, respectively. Boundary conditions on the conducting wall are described as follows with a normal unit vector $\boldsymbol{n}$:

$$\boldsymbol{n} \cdot \boldsymbol{H} = \boldsymbol{0}, \ \boldsymbol{n} \times \boldsymbol{E} = \boldsymbol{0} \text{ on } \Gamma. \tag{21}$$

In the cylindrical coordinates (r, θ, z), An analysis of an axisymmetric resonant cavity is reduced to the following axisymmetric scalar Helmholtz equation in two dimensional coordinates (r, z) [8], [9]:

$$L\phi = -k^2\phi, \quad L \equiv r\frac{\partial}{\partial r}\left(\frac{1}{r}\frac{\partial}{\partial r}\right) + \frac{\partial^2}{\partial z^2}. \tag{22}$$

Definitions of ϕ and boundary conditions become

$$\phi \equiv rE_\theta \ \text{ and } \ \overline{\phi}_\Gamma = 0 \text{ on } \Gamma \text{ for TE mode,}$$

$$\phi \equiv rH_\theta \ \text{ and } \ \overline{q}_\Gamma = 0 \text{ on } \Gamma \text{ on TM mode.} \tag{23}$$

The integral equation is obtained in the IEM formulation [8], [9], [12]:

$$C_{i}\phi_i + \int_\Gamma \frac{\phi}{r}\frac{\partial \phi^*}{\partial n}\,d\Gamma - \int_\Gamma \frac{\phi^*}{r}\frac{\partial \phi}{\partial n}\,d\Gamma = k^2\int_\Omega \frac{\phi\phi^*}{r}\,d\Omega. \tag{24}$$

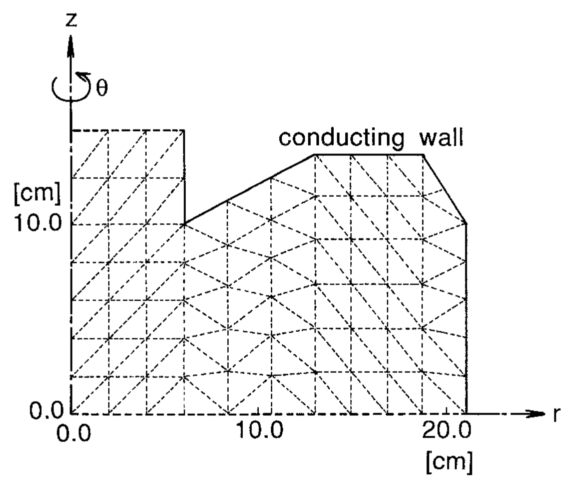

Fig. 5. Division of the axisymmetric model of the PETRA accelerating cavity [1] in the cylindrical coordinates.

In (24), ϕ^* is the following fundamental solution for the source point (r', z'):

$$\phi^* = \frac{\sqrt{rr'}}{\pi p}\left[\left(1 - \frac{p^2}{2}\right)K(p) - E(p)\right],$$
$$p^2 = \frac{4rr'}{(r + r')^2 + (z - z')^2}, \quad (25)$$
$$\frac{1}{r}L\phi^* + \delta(r - r')\,\delta(z - z') = 0,$$

where $K(p)$ and $E(p)$ are, respectively, the complete elliptical integral functions of the first kind and second kind. These integral functions are evaluated with high accuracy and short computational time by using mathematical libraries of computer systems [12]. In the analysis of a resonant cavity, the second IEM formulation is suitable and (10), (11) become the following from the boundary conditions in (23):

$$[\boldsymbol{P}]\{e_\Gamma\} = k^2[\boldsymbol{S}']\{\phi_\Omega\}, \quad (26)$$
$$\{\phi_i\} = [\boldsymbol{E}]\{e_\Gamma\} + k^2[\boldsymbol{T}']\{\phi_\Omega\}, \quad (27)$$

where the wave number k is arranged in front of the matrices $[\boldsymbol{S}']$ and $[\boldsymbol{T}']$. Then the following characteristic equation is obtained from (26), (27) [8], [9]

$$[\boldsymbol{A}]\{\phi_\Omega\} = \beta\{\phi_\Omega\},$$
$$[\boldsymbol{A}] \equiv [\boldsymbol{E}][\boldsymbol{P}]^{-1}[\boldsymbol{S}'] + [\boldsymbol{T}'], \quad \beta \equiv k^{-2}. \quad (28)$$

Eigenvalues and eigenfunctions are obtained from (28) with a standard numerical technique. They correspond to the resonant wave numbers and the internal potentials respectively. Fig. 5 shows a division of the 1/4 axisymmetric model of the PETRA accelerating cavity [1]. A solid line of the boundary shows the conducting wall and the model is divided to 123 elements. Several resonant frequencies are calculated as shown in Table I. The IEM solutions agree well with the FDM solutions [1]. In this way, the analysis of a resonant cavity is reduced to the simple eigenvalue problem and the determinant search method is not needed in the IEM.

TABLE I
COMPARISONS OF RESONANT FREQUENCIES OF THE PETRA ACCELERATING CAVITY [1]

Modes	FDM Solutions [MHz] [1]	IEM Solutions [MHz]
TM0-EE-1	515.2	514.2
TM0-EE-2	1247.2	1243.6
TM0-EM-1	515.6	514.7
TM0-EM-2	1266.6	1244.2
TM0-MM-1	757.0	753.2
TM0-MM-2	1477.1	1444.2

One of difficulties of the BEM analyses for axisymmetric Helmholtz-type equations is that fundamental solutions of many axisymmetric Helmholtz-type equations are obtained not by closed forms but by integral forms [12]. Application of the IEM to the problems is useful since the fundamental solution is obtained by the well known closed form in (25).

IV. Conclusion

In the paper, scalar Helmholtz equations are solved with the IEM. Further study on the vector Helmholtz equation will be carried out in the near future. Results in the paper are summarized as follows.

1) Two IEM formulations are obtained for the scalar Helmholtz equation. One is a standard formulation and the other is obtained from an elimination of unknown boundary values.

2) Two dimensional scalar Helmholtz equations are analyzed by the IEM and the FEM. Both solutions are in good agreement with exact solutions. Though the IEM requires considerable computational time compared with the FEM, the first derivative is obtained directly with high accuracy.

3) An axisymmetric resonant cavity is analyzed with the second IEM formulation. The problem is reduced to an analysis of the simple characteristic equation, and the IEM solutions agree well with the FDM solutions.

References

[1] T. Weiland, "On the computation of resonant modes in cylindrically symmetric cavities," *Nucl. Instrum. Methods.*, vol. 216, pp. 329–348, 1983.
[2] J. B. Davies, F. A. Fernandez, and G. Y. Philippou, "Finite element analysis of all modes in cavities with circular symmetry," *IEEE Trans. Microwave Theory Tech.*, vol. 30, pp. 1975–1980, 1982.
[3] M. Hara, T. Wada, T. Fukasawa, and F. Kikuchi, "A three dimensional analysis of RF electromagnetic fields by the finite element method," *IEEE Trans. Magn.*, vol. 19, pp. 2417–2420, 1983.
[4] J. H. Whealton *et al.*, "A 3D analysis of Maxwell's equations for cavities of arbitrary shape," *J. Comput. Phys.*, vol. 75, pp. 168–189, 1988.
[5] Y. Kagawa *et al.*, *Finite Element and Boundary Element Methods for Electrical Engineering*, Ohm Publishing, Tokyo, sec. 2.1, 1984, in Japanese.
[6] N. Tosaka and K. Kakuda, "New integral equation method for approximate solution of eigenvlaue problems," *Trans. Architectural Inst. Japan*, vol. 328, pp. 36–43, 1983, in Japanese.

[7] ——, "An integral equation method for non-self-adjoint eigen value problems and its applications to non-conservative stability problems," *Int. J. Num. Meth. Eng.*, vol. 20, pp. 131-141, 1984.
[8] M. Tsuchimoto, T. Honma, and A. Yoneta, "Boundary element analysis of axisymmetric resonant cavities," *IEEE Trans. Magn.*, vol. 24, pp. 2500-2503, 1988.
[9] M. Tsuchimoto and T. Honma, "An analysis of axisymmetric resonant cavities by using the hybrid boundary element method," *Trans. IEICE Japan*, vol. E-71, pp. 301-303, 1988.
[10] S. H. Wong and Z. J. Cendes, "Numerically stable finite element methods for the Galerkin solution of eddy current problems," *IEEE Trans. Magn.*, vol. 25, pp. 3019-3021, 1989.
[11] Y. Saito, Y. Nakazawa, and S. Hayano, "Non-spurious finite element solution of eddy current problems," *Rep. of IEE Japan*, SA-90-20, pp. 61-70, 1990, in Japanese.
[12] M. Tsuchimoto, K. Miya, T. Honma, and H. Igarashi, "Fundamental solutions of the axisymmetric Helmholtz-type equations," *Appl. Math. Modelling*, vol. 14, pp. 605-611, 1990.

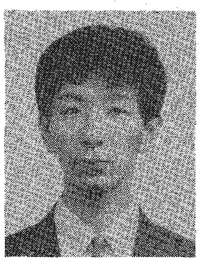

Masanori Tsuchimoto was born in Tokyo, Japan, on May 1, 1961. He received the M.E. degree in electrical engineering from Hokkaido University in 1987.

He is currently a Research Associate at the Nuclear Engineering Research Laboratory, Faculty of Engineering, University of Tokyo. His research interests include numerical analyses and experiments of electromagnetic field problems.

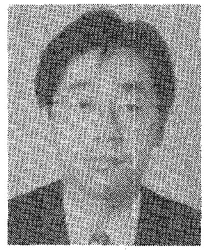

Atsuhiko Yoneta was born in Hokkaido, Japan on April 20, 1964. He received the M.E. degree in electrical engineering from Hokkaido University in 1990.

He is now with NTT Data Communication Systems Corporation, Tokyo, Japan. His research interests include the area of electromagnetics interference theory and numerical method applied to printed circuit board.

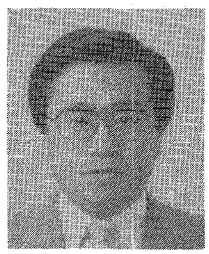

Toshihisa Honma was born in Hokkaido, Japan on Sept. 26, 1947. He received the Dr.E. in electrical engineering from Hokkaido University, Japan in 1976. Since 1987 he has been a Professor in the Department of Electrical Engineering, Faculty of Engineering, Hokkaido University. He has been engaged in research in the field of computational electromagnetics, applied electromagnetics, plasma physics, nuclear fusion engineering, electromagnetic propulsion engineering, charged particle beams and micro gravity engineering. His research interests include application of the boundary element method to electrical engineering problems now.

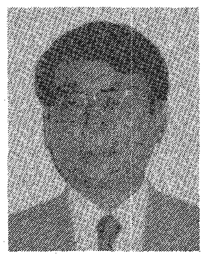

Kenzo Miya was born in Nagasaki, Japan, on June 13, 1940. He received the Dr.E. degrees in nuclear engineering from the University of Tokyo, Japan in 1969.

Since 1983 he has been a Professor at Nuclear Engineering Research Laboratory, Faculty of Engineering, University of Tokyo. From 1978 to 1979 he was a Guest Professor at the University of Maryland. In 1980 he was a Guest Professor of Cornell University. He has been engaged in the research fields of structural mechanics, nuclear fusion engineering, and applied electromagnetics.